2018

Rheological Characterization of Fluids for Lithium Ion Batteries and Thermal Ablation of Tumors

Joseph P. Sullivan
University of Rhode Island, josephsullivan@uri.edu

RHEOLOGICAL CHARACTERIZATION OF FLUIDS FOR LITHIUM ION BATTERIES AND THERMAL ABLATION OF TUMORS

BY

JOSEPH P SULLIVAN

A THESIS SUBMITTED IN PARTIAL FULFILLMENT OF THE

REQUIREMENTS FOR THE DEGREE OF

MASTER OF SCIENCE

IN

CHEMICAL ENGINEERING

UNIVERSITY OF RHODE ISLAND

2018

MASTER OF SCIENCE THESIS

OF

JOSEPH P SULLIVAN

APPROVED:

Thesis Committee:

Major Professor Arijit Bose

Daniel Roxbury

Brett Lucht

Nasser H. Zawia
DEAN OF THE GRADUATE SCHOOL

UNIVERSITY OF RHODE ISLAND
2018

ABSTRACT

Rheology is the study of the flow of matter. To determine what material is most suitable for an application involving material flow, an instrument called a rheometer can characterize material behavior under specific conditions. A variety of procedures can be used to determine the properties of a fluid when it is heated, stressed, or mixed with another fluid. This study uses a stress controlled rheometer to characterize the response of various fluids to conditions expected in their related processes. These responses are analyzed and results are organized into three manuscripts.

The first manuscript investigates the behavior of lithium ion battery anode components in a new method of anode production called emulsion templated directed assembly. This method uses carbon black nanoparticles to contain a silicon-rich oil phase inside of a polymer-rich water phase. The rheological properties of carbon black and reduced graphene oxide suspensions in water were recorded at a range of pH levels. These results were compared to suspensions including polymer binder. It was determined that the water phase of an anode produced by emulsion templating would not develop an interconnected network prior to the drying process, and the inclusion of a polymer binder has minimal effect on system viscosity.

The second manuscript determines the viscoelastic properties of graphite lithium ion battery anode slurries containing Timcal Super P or Cabot LITX-50, two common carbon black additives. Super P appears to create a slurry that is easier to manufacture with and less likely to suffer from cracks while drying than a slurry with LITX-50.

In the third manuscript, rheological characterization and viscosity measurements were made for several thermal accelerant solutions. Thermal accelerant is designed to deliver as a solution into the liver with sufficient viscosity to remain stationary at a target site during ablation. After the rheological characterization of a series of the thermal accelerant solutions, the sample designated “TA 50” appears to meet these criteria most effectively.

ACKNOWLEDGMENTS

I would like to express my deep gratitude to Dr. Bose for his guidance and insight throughout this past year. The work contained in these pages presented an opportunity for personal and academic growth for which I will always be grateful. With his support, what once was a turbulent maelstrom of observations, charts, and notes has been streamlined into a laminar flow of thought.

I also thank Dr. William Keun Chan Park for the chance to collaborate with his laboratory group. I maintain the utmost respect for his field of study, and I am grateful for an opportunity to participate in some small way.

PREFACE

This thesis has been prepared in Manuscript Format.

“πάντα χωρεῖ καὶ οὐδὲν μένει”

“δὶς ἐς τὸν αὐτὸν ποταμὸν οὐκ ἂν ἐμβαίης”

- Ἡράκλειτος ὁ Ἐφέσιος

TABLE OF CONTENTS

LIST OF FIGURES

FIGURE PAGE

MANUSCRIPT – I

Rheological Characterization of Carbon Black and Reduced Graphene Oxide Suspensions for Lithium Ion Battery Anodes

In preparation, to be submitted to ACS Langmuir as:

Microstructural and Rheological characterization of Aqueous Suspensions of Carbon Black and Reduced Graphene Oxide

Yuzi Zhang, Joseph P. Sullivan, Arijit Bose

Chemical Engineering, University of Rhode Island, Kingston, RI, USA

Corresponding Author: Arijit Bose, Ph.D.

Chemical Engineering

University of Rhode Island

129 Pastore Hall, 51 Lower College Rd.

Kingston, RI, 02881, USA

Phone: +1-401-874-2804

Email address: bosea@uri.edu

Abstract

Silicon is an attractive anode material for lithium ion batteries due to its high theoretical capacity to store lithium, but expansion and contraction present during charge and discharge have hindered its use. In a process called emulsion templated directed assembly, carbon black, augmented by reduced graphene oxide, is able to encapsulate silicon, preventing damage to the anode. Carbon beyond what is required to encapsulate the silicon forms a conducting network to carry electrical charge. The viability of this anode depends on the strength of the carbon network and the polymer binder that supports it. This study characterized the rheological properties of aqueous carbon black and reduced graphene oxide suspensions at a range of pH levels, and compared these results to suspensions including polymer binder. It was determined that the water phase of an anode produced by emulsion templating would not develop an interconnected network prior to the drying process, and the inclusion of a polymer binder has minimal effect on system viscosity.

Introduction

Today, lithium ion batteries (LIBs) are produced on the order of billions of units per year.[1] One major point of study in the current generation of LIBs is the development of a new anode material.[2] Current LIBs typically use graphite anodes. Graphite has a layered structure, allowing lithium ions to intercalate between the layers during charging and leave the layers during discharge. The theoretical capacity of graphite to store lithium is approximately 372 mAh/g,[3,4] too low for applications such as electric vehicles. Silicon has been proposed as a new anode material due to its high theoretical specific capacity of 4,200 mAh/g.[4] While the usefulness of an electrode is mainly determined by its lithium ion capacity and cycle stability, all of the energy output of a battery derives from electron conduction. To that end, conducting carbon is added to the anode as well as the cathode, as silicon and many cathode materials are poor electron conductors. To carry this charge to the charge collector, various conducting networks have been proposed, including carbon coatings,[5] nanotube composites,[6,7] and nanowires.[8]

Although silicon has a large theoretical capacity, when used as an anode material in a LIB, it undergoes substantial volumetric strain of about 270% during charge, and the reverse during discharge.[9] With repeat cycling, this volume expansion and contraction can lead to pulverization of the particles, exposing fresh surfaces to the electrolyte. A solid electrolyte interphase forms at these surfaces, irreversibly consuming lithium ions and leading to capacity loss. An additional issue is that the volume expansion and contraction is relayed to the electron conducting network, often breaking it, and reducing electron conduction. The conducting network must either be

able to absorb the stress incurred during lithiation while maintaining its elasticity after delithiation, or be supported by a binding agent that can do so.

Since the conducting carbon does not contribute towards the capacity of the electrode, reduction of the carbon weight percent in an anode is one way to lower the overall weight of and raise the overall energy density in an LIB. It is therefore important to find a minimum amount of carbon required to form an effective conductive network. This minimum must be one that also limits destruction of the network during lithiation and delithiation to prevent the capacity of the battery from fading rapidly over time.

The first step in the assembly of a cell is the deposition of a suspension containing the active material, conducting material and binder in a solvent on to a copper film or on an aluminum film. A doctor blade is used to remove excess material. The slurry is then dried, calendared and sized. The rheological characteristics of the suspension have a strong impact on the thickness of the deposited layer.[14, 15] Suspension rheology will also affect the final thickness of the layer after the drying process.[14-16] In addition, differential capillary stresses in the electrodes during drying must be absorbed, so that cracks do not develop.[17] The rheological characteristics of the suspension can thus impact several parts of the electrode fabrication process. The major goal of this work is to thoroughly characterize the rheological properties of a suspension used in our own work for preparing anodes, as well as a suspension commonly used in commercial anodes for lithium ion batteries.

Para-amino benzoic acid terminated carbon black (CB) is a fractal particle that will form a network in solution. An emulsion of stabilized by particles such as CB is

called a Pickering emulsion. In contrast to a classical emulsion, in which the dispersed phase tends to coalesce over time, a Pickering emulsion will remain stable.[10] At concentrations higher than that required to form the network, the particles will disperse within the aqueous phase. This network shows promise in LIBs as a charge carrier when prepared during emulsion-templated directed assembly.[11] When a silicon rich oil phase is emulsified into an aqueous phase and dried, the silicon particles are encaged by a carbon network. The cage allows for silicon expansion and contraction, while the network provides support during lithiation and delithiation. It has also been shown that reduced graphene oxide (RGO) can act as an effective substitute for CB while reducing the total amount of carbon required to form a conducting network.[12] Its behavior alongside carbon black at varying concentrations is of interest for this study.

Before the drying process, polymer binder is present in the water phase of LIB anodes produced using the emulsion-templated directed assembly method.[11] Rheological characterization of the binder may provide insight to its behavior while drying and the behavior of the anode slurry during deposition.

Materials and Methods

Sample Preparation:

A 15 wt% stock suspension of para-amino benzoic acid (PABA)-terminated carbon black (CB) in water at pH 7 was provided by Cabot Corporation. Reduced graphene oxide nanoplatelets (RGO) with a specific surface area of ~833 m^2/g and carbon/oxygen ratio of 10.5:1 were purchased from Graphene Supermarket. These RGO particles have an average lateral dimension of ~4 μm and thickness ~3-4 nm. 37 wt% hydrochloric acid (HCl) was purchased from Sigma Aldrich. Deionized water was obtained from a Millipore Milli Q system. CB and RGO samples were created for CB concentrations ranging from 0 - 10 wt%, RGO concentrations of 0.01 wt% and 0.05 wt%, and a pH range of 3 – 7.

Polymer binder solutions were created through the same materials and methods in [12]. Binder characterization began with the stock binder solution, consisting of a 20mg/ml mixture of 1:1 weight ratio CMC to PAA. This solution was added to samples with and without CB. All binder solutions were pH 3.3.

Rheology:

Characterization was completed by a TA Instruments AR-2000 stress controlled rheometer. A cone and plate geometry was utilized. This configuration had a set minimum gap height of 51 μm, a cone angle of 2°, and a cone diameter of 4 cm. The gap is much larger than the minimum particle size. All experiments were done at 25 C.

Samples were first probed for a change in viscosity with respect to shear rate, ranging from 3 s^{-1} to 2000 s^{-1}. Each experiment began with a preshear of 10 s^{-1} for 120 seconds to remove stresses incurred during sample loading. Viscosity characterization was performed three times for each sample.

Some samples were also probed for viscoelastic response. A determination of the appropriate range of stress for each sample is required before oscillatory response can be obtained. Within this range, called the linear viscoelastic region (LVR), the stress varies linearly with strain. Outside of the LVR, the stress applied damages the sample. To find the LVR, stress is applied to the sample in a one second cycle. The resulting strain is measured throughout the cycle and the lag time between the application of the stress and strain response is calculated. Graphically, a purely viscous liquid would exhibit a $\delta = 90^{o}$ offset in strain response for an applied stress, whereas a purely elastic solid would show a strain response immediately to an applied stress and a phase shift of $\delta = 0^{o}$. The solid-like portion of the response is displayed as the Storage Modulus (G') and the liquid-like portion is displayed as the Loss Modulus (G"). The relationship between stress, strain, and moduli can be represented as:

$$\sigma(t) = \gamma_0[G'(\omega)\, sin(\omega t) + G"(\omega) cos(\omega t)]$$

Where σ is the shear stress produced, ω is the angular frequency of oscillation, and γ_0 is the amplitude of the strain imposed on the fluid.[18] If the strain amplitude is small, the structure of the fluid will not be affected by the oscillatory measurement. Shear stress output measured by the rheometer is converted to G' and G" contributions after each cycle of increasing applied strain. When G' and G" are no longer constant as strain increases, the sample is no longer in the LVR. For convenience, stain

amplitude is converted to oscillatory stress by the rheometer software, and the LVR is presented as the moduli as functions of oscillatory stress.

Once the LVR was determined for a sample, it was vortexed at 3000 rpm for 30 seconds. Each sample was probed within three minutes of vortexing. A 0.1 rad/s preshear was utilized for the oscillatory sweep. G' and G" were calculated for angular frequencies from 0.01 to 100 rad/s at an oscillatory stress within the LVR.

In some cases, an increase in viscosity or modulus response may be present in the results at the highest shear rates or angular frequencies, respectively. This effect does not necessarily indicate shear thickening behavior or a change in microstructure; a response uptick at high instrument speed is likely due to contributions of the rotating geometry. Viscosity and modulus are each calculated from a measured torque value. For dilute aqueous suspensions at high shear rate, secondary toroidal flows are present. This leads to a higher torque requirement to maintain a given rate of shear, and can be falsely interpreted as a higher measured viscosity. Similarly, the torque required to oscillate the cone at 100 rad/s is considerably greater than the amount of torque contributed by particle interactions in a dilute aqueous suspension. In both cases, high shear results should not be considered when determining fluid behavior.

Results and Discussion

Carbon Black Weight Percentage:

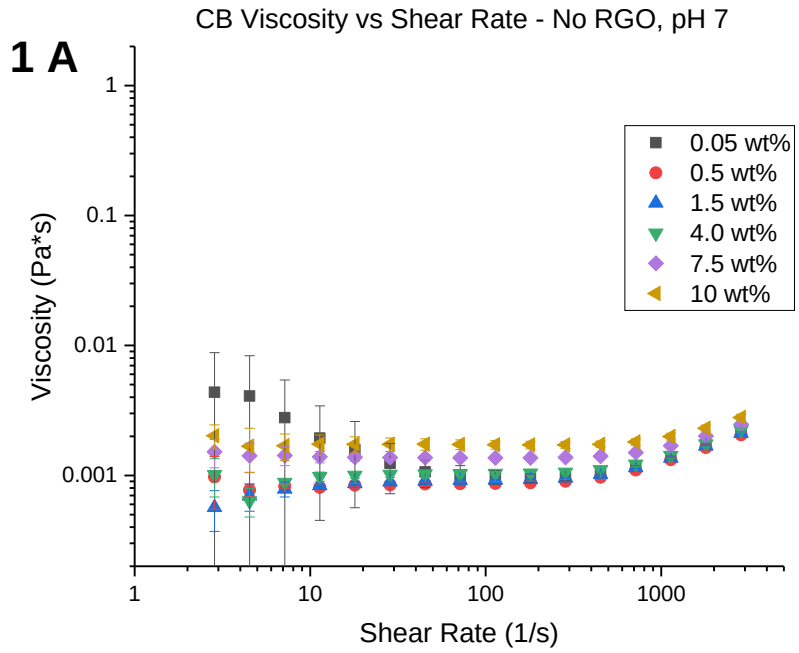

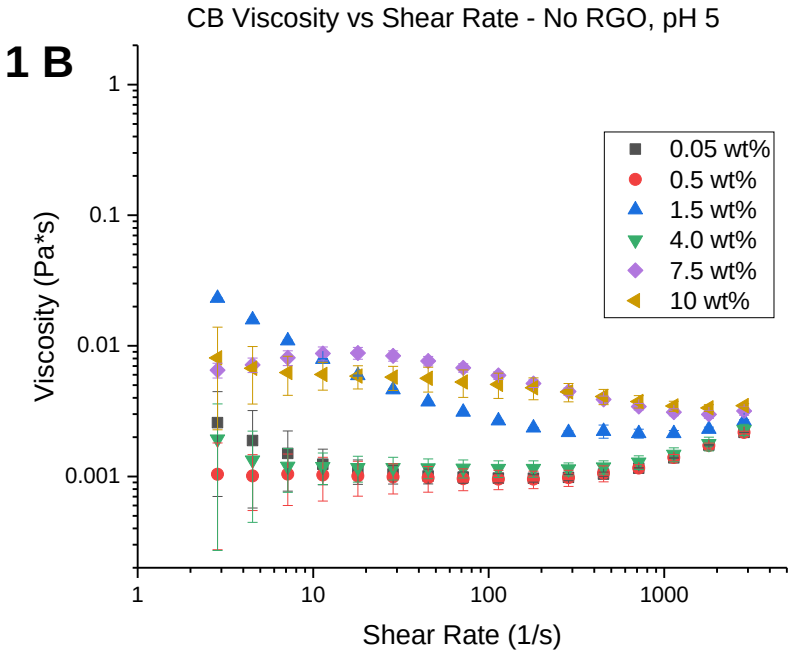

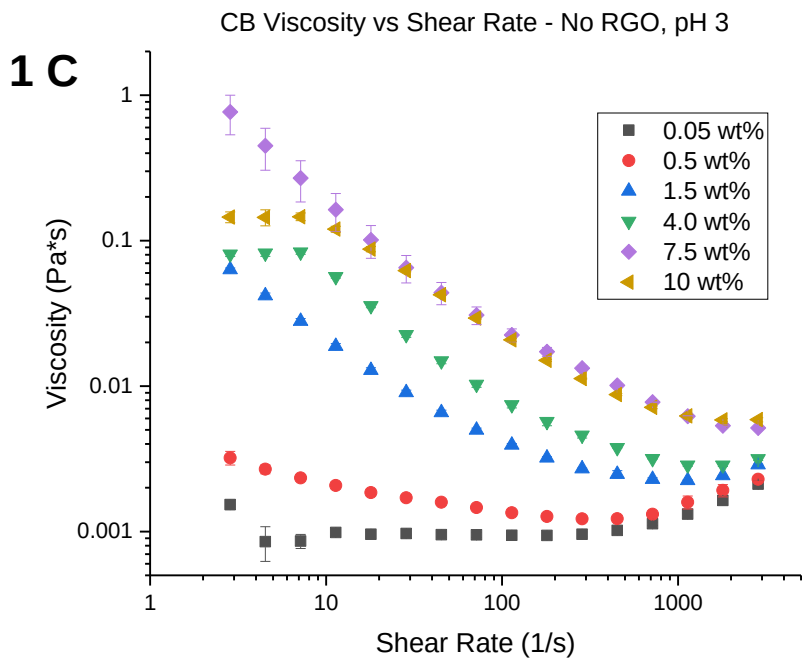

Fig. 1: Viscosity response of samples containing carbon black to shear at (a) 7, (b) 5, and (c) 3 pH

Figure 1 shows the viscosities of CB concentrations without RGO at pH 3, 5, and 7. Shear thinning behavior is not present for any CB loading at pH 7. The variance in viscosity at low shear rates is within the error expected for a fluid with a viscosity similar to that of water, 0.8×10^{-3} Pa*s at 25 C, especially with a cone and plate geometry. Reduction of sample pH to 5 increased viscosity in the 10 wt% and 7.5 wt% CB solutions, which reduce to a Newtonian plateau at high shear rates. At pH 3, shear thinning is present in CB solutions from 1.5 wt % to 10 wt%. The solution viscosity increases with CB wt%, with the exception of 10 wt% CB. Here, the 10 wt% solution is less viscous than the 7.5 wt% CB sample.

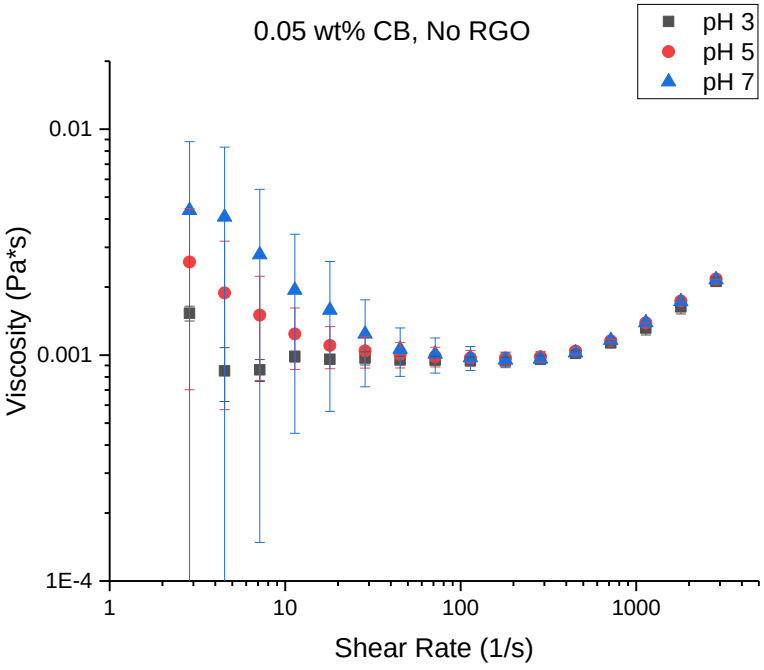

Fig. 2: 0.05 wt% CB without RGO

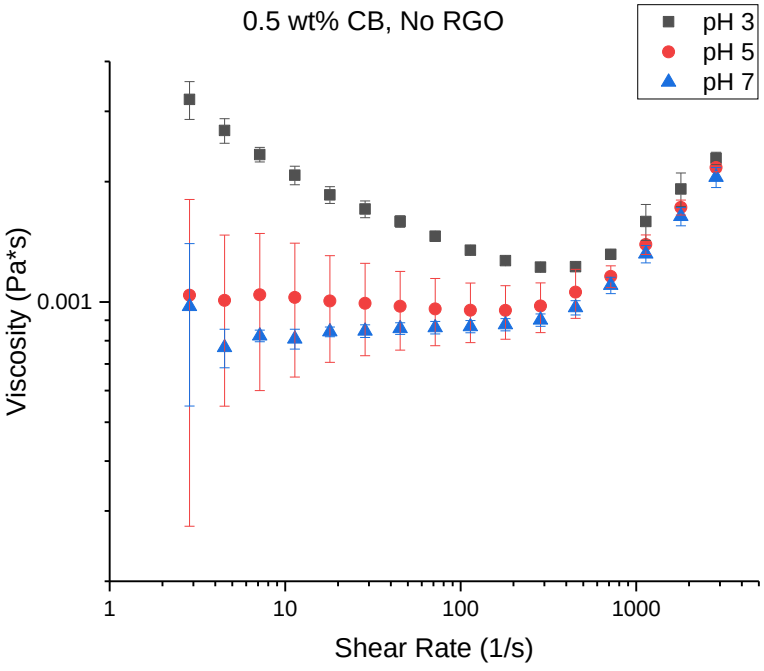

Fig. 3: 0.5 wt% CB without RGO

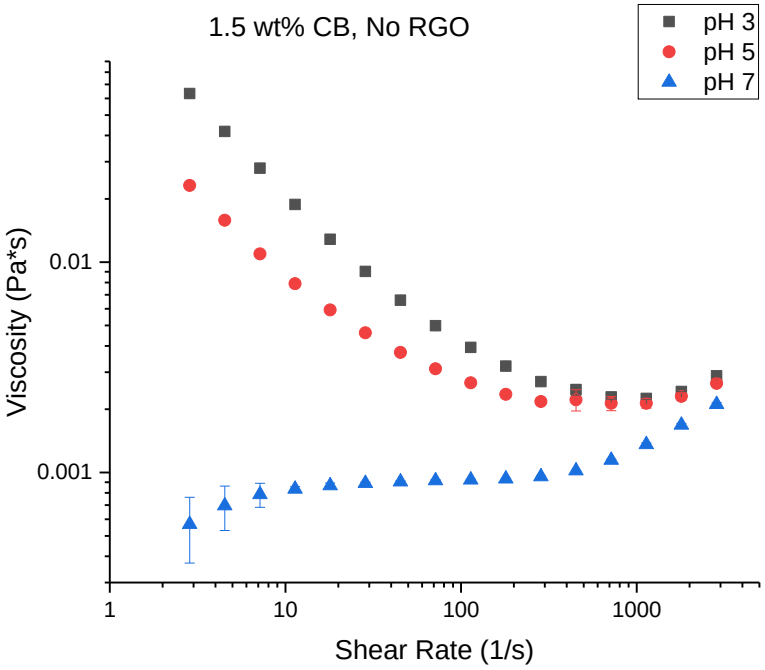

Fig. 4: 1.5 wt% CB without RGO

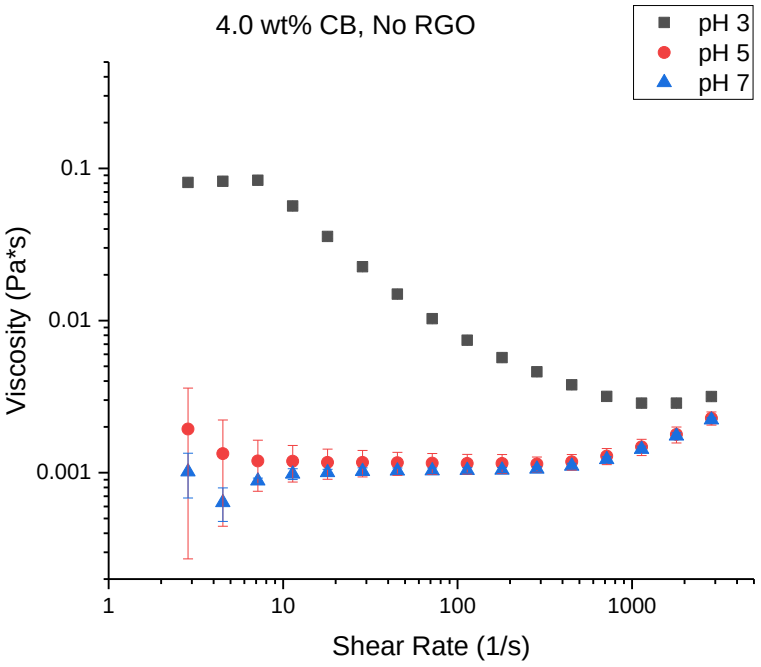

Fig. 5: 4.0 wt% CB without RGO

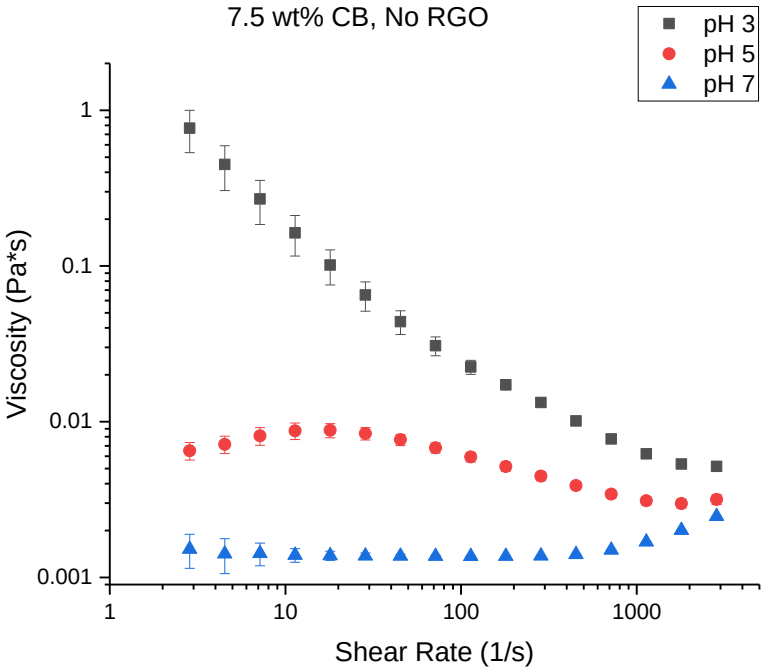

Fig. 6: 7.5 wt% CB without RGO

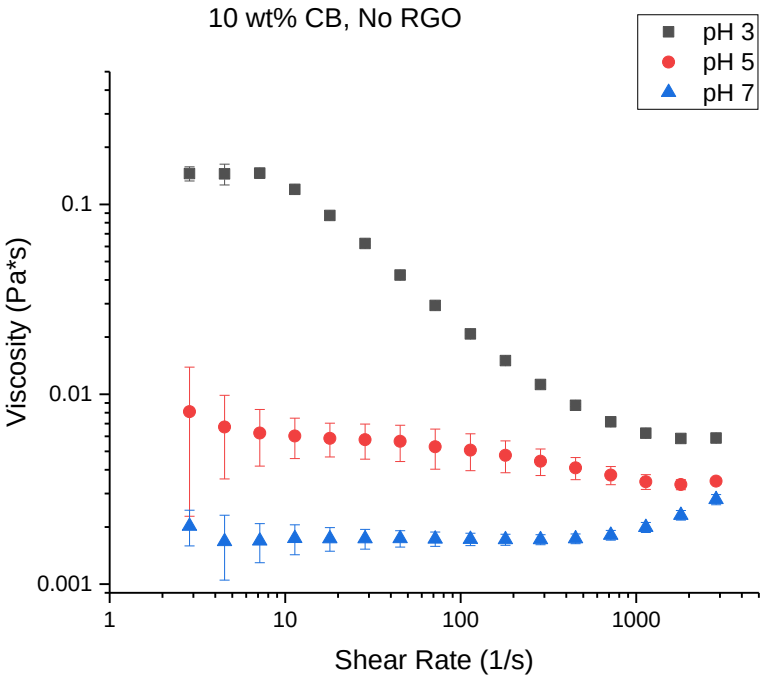

Fig. 7: 10 wt% CB without RGO

As shown in Figures 2-7, viscosity of the CB-only suspensions tends to increase as pH decreases. The pH dependence of viscosity for CB is largely due to the surface carboxylate groups present in the PABA-terminated CB. It has been shown that these carboxyl groups protonate as pH lowers, and the particles become increasingly hydrophobic.[13] It is energetically unfavorable for these hydrophobic regions to be exposed to water, so they connect with each other and form a network, increasing the suspension viscosity for a given CB concentration. At high CB loadings, it is possible that these aggregates become too large to support network formation.

In all cases where shear thinning behavior is present, the viscosity of the carbon samples is greater than the Einstein prediction for the corresponding volume fraction. Here, this relation is given as:

$$\eta_{suspension} = \eta_{solvent} * (1 + 2.5\phi)$$

Where $\eta_{solvent}$ is the viscosity of water at 25°C, and ϕ is the volume fraction of CB.[19] The range of 0.05 wt% to 10 wt% equates to a range of 2.3×10^{-4} Pa*s to 4.5×10^{-2} Pa*s for the ϕCB of these samples.

Reduced Graphene Oxide:

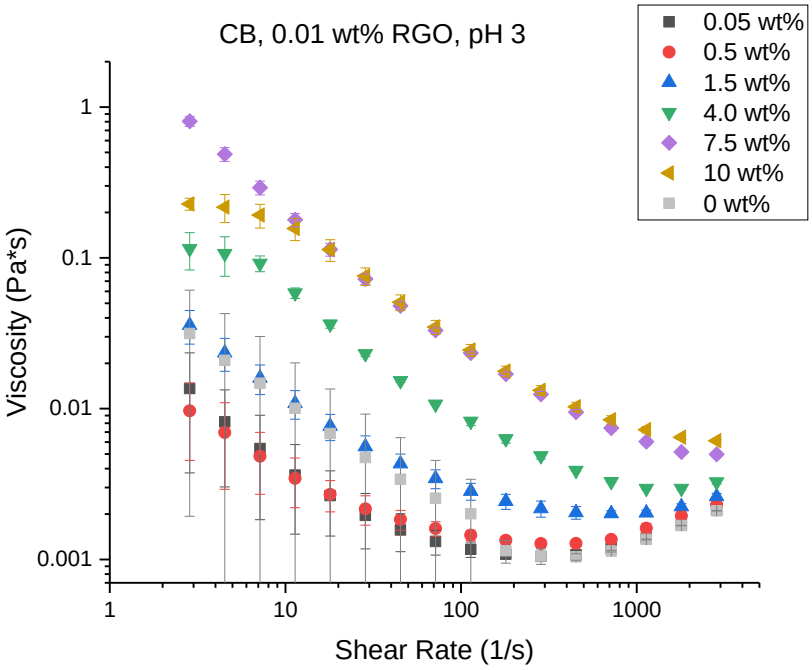

Fig. 8: CB with 0.01 wt% RGO at pH 3

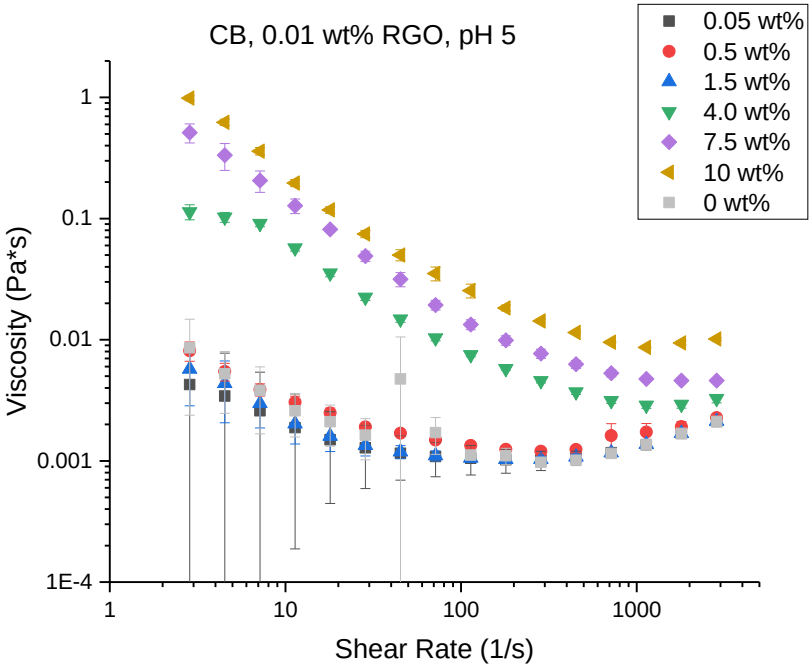

Fig. 9: CB with 0.01 wt% RGO at pH 5

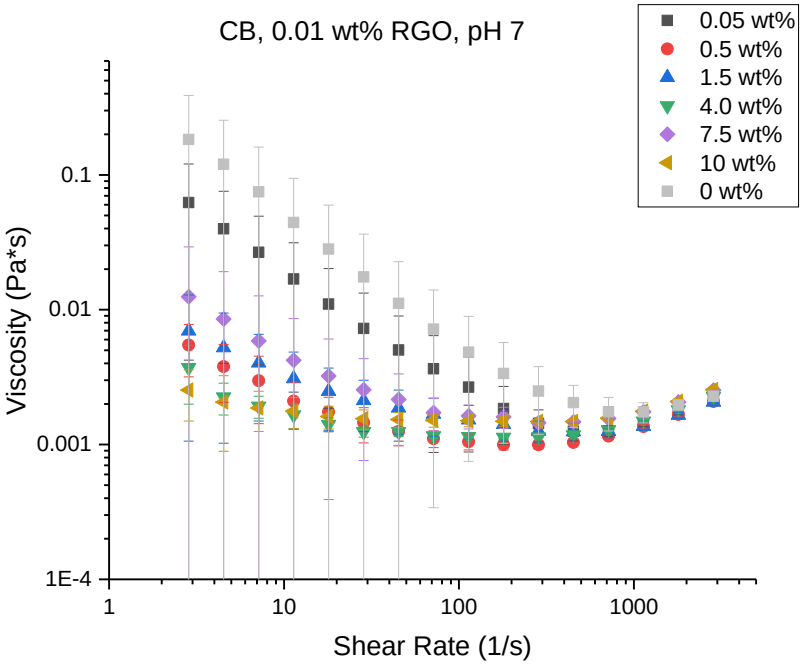

Fig. 10: CB with 0.01 wt% RGO at pH 7

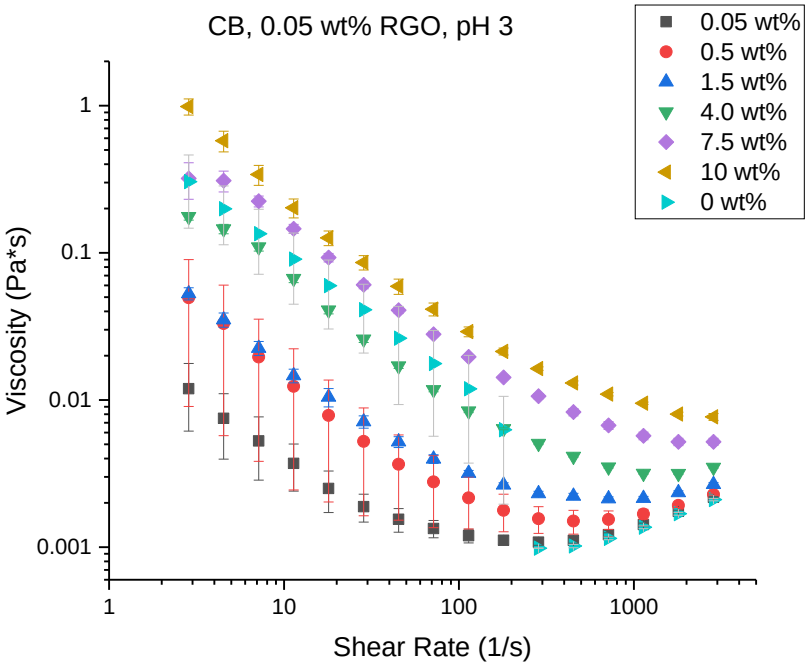

Fig. 11: CB with 0.05 wt% RGO at pH 3

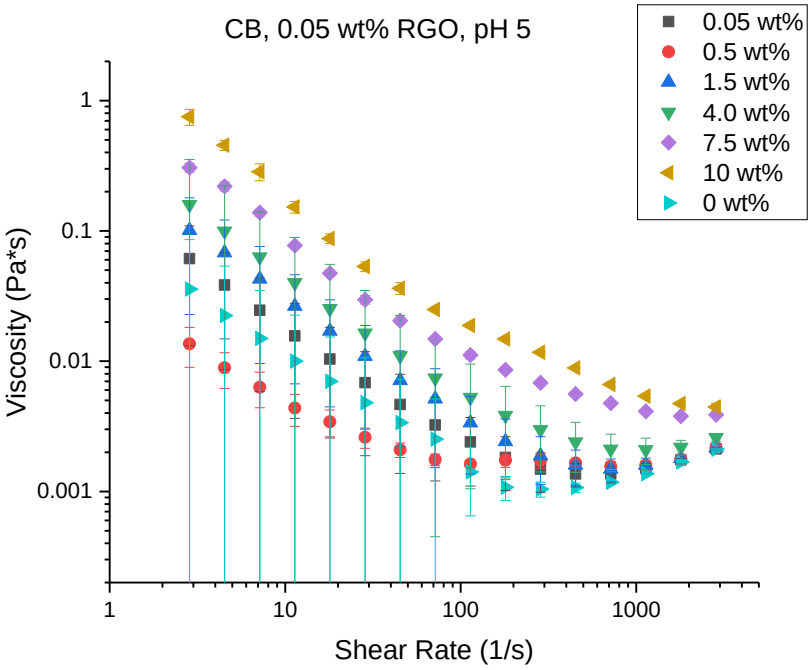

Fig. 12: CB with 0.05 wt% RGO at pH 5

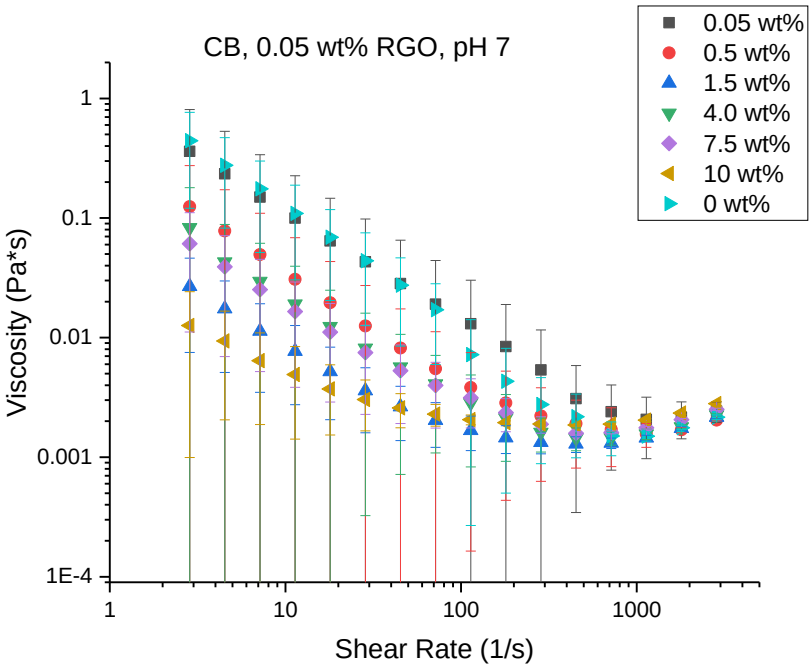

Fig. 13: CB with 0.05 wt% RGO at pH 7

Dependence of solution viscosity on RGO concentration was investigated for the range of CB loadings at pH 3, 5, and 7. As shown in Figures 8 and 9, the addition of 0.01 wt% RGO tends to increase the viscosity of pH 5 samples towards the pH 3 upper limit. This effect increases with increasing CB wt%. Similarly, addition of 0.05 wt% RGO led to a consistent increase in low shear viscosity at all CB wt% for the pH 7 samples. At pH 3, only CB loadings below 1.5 wt% are affected by RGO content. Overall, addition of RGO appears to increase the viscosity of low CB loadings while pH decrease increases the viscosity of high CB loadings.

Oscillatory Response of CB and RGO Suspensions in Water:

Oscillatory characterization was performed on all pH 3 CB and RGO samples to further investigate CB and RGO network formation. Meaningful results were not obtained for any carbon loading; the magnitudes of the moduli were not large enough to suggest a prevailing microstructure was present in any sample.

Polymer Binder:

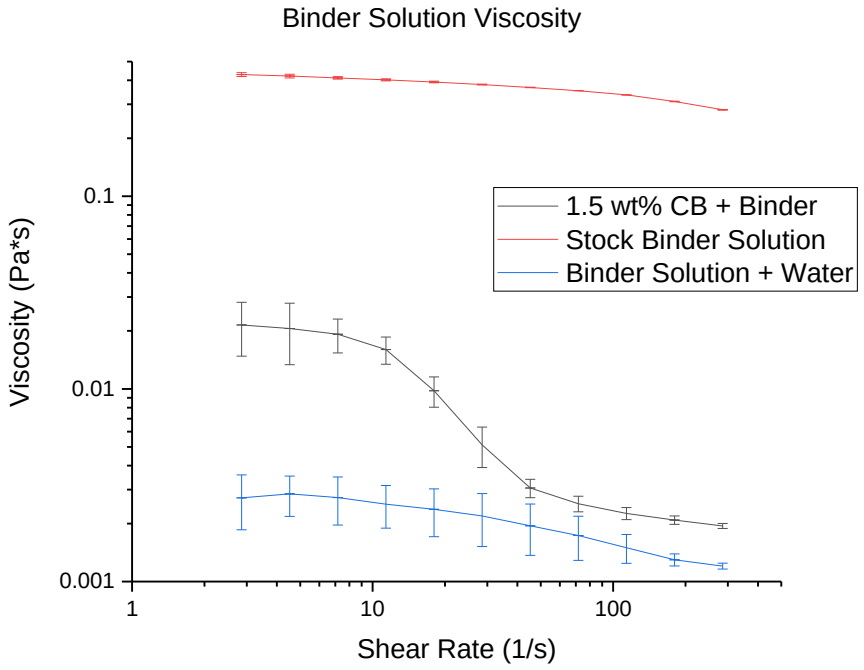

Fig. 14: Viscosity of solutions with polymer binder

Binder solution viscosities are shown in Fig. 4. The stock solution (red line) is a Newtonian liquid nearly three orders of magnitude more viscous than water, while the dilution (blue line) is Newtonian and approximately as viscous as water. Addition of 1.5 wt% CB to the dilution increases the solution viscosity considerably, particularly at high shear.

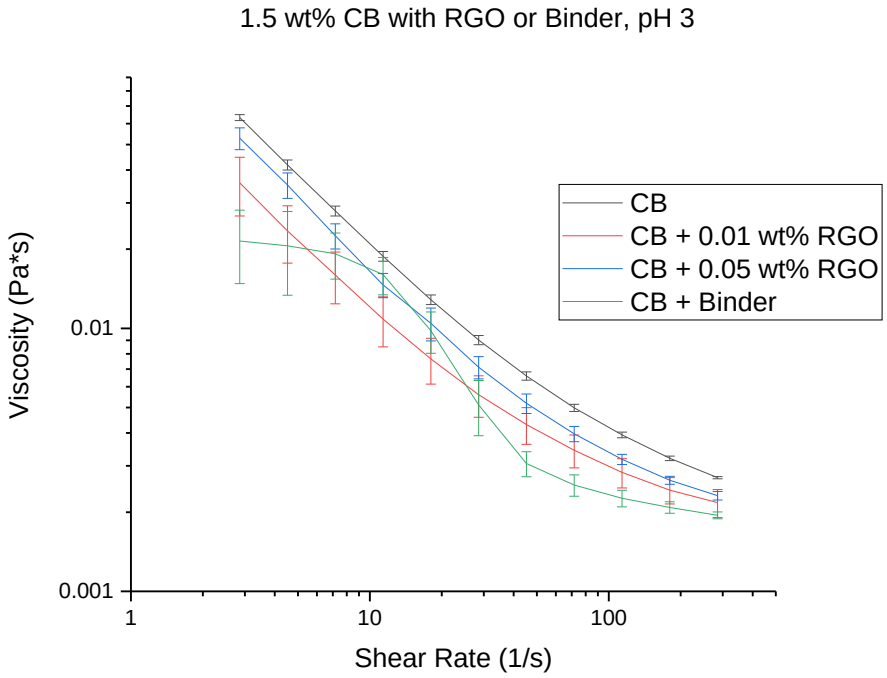

Fig. 15: Viscosity for 1.5 wt% CB with and without RGO and binder

The viscosity of the CB with binder falls within the range of viscosity measurements on all 1.5 wt% CB RGO loadings, shown in fig. 5. Although the binder addition results in the development of a low shear Newtonian plateau, the viscosity difference is within the range of expected values for all compositions. Although samples of 0.14 wt% and 0.26 wt% CB were used in the anodes in [12], 1.5 wt% CB was chosen for the comparison due to its higher viscosity. The results from Figure 1A show that 0.05 wt% and 0.5 wt% CB are subject to large variances from rheometer limitations. 1.5 wt% CB has considerably less variance, but is the lower limit of the reliable data.

Oscillatory characterization could not be performed on the dilution, with or without CB, as no stable LVR was present.

Conclusions

The viscosity dependence of aqueous suspensions of carbon black and reduced graphene oxide on carbon content and pH has been shown. Generally, as pH increases, addition of RGO to a suspension will increase the viscosity for low CB loadings, with diminishing effect as CB wt% increases. None of the suspensions in this study exhibit viscoelastic properties indicating the presence of a network throughout the water phase. This suggests that the water phase of an anode produced by emulsion templating would not develop an interconnected network prior to the drying process.

Inclusion of a polymer binder has minimal effect on system viscosity. This has been shown for 1.5 wt% CB, which is considerably more concentrated than the solutions in [12]. Although the determination of binder influence was completed at higher CB wt% due to instrument limitations, it suggests that even at lower CB concentrations, the contribution of the binder to the bulk rheological properties of the water phase in emulsion templated directed assembly may be minimal.

References

(1) Scrosati, B.; Garche, J. Lithium batteries: Status, prospects and future. *Elsevier Journal of Power Sources* **2010**, *195* (9), 2419-2430

(2) Goodenough, J.; Park, K.-S. The Li-Ion Rechargeable Battery: A Perspective. *J. Am. Chem. Soc.* **2013**, *135* (4), 1167-1176.

(3) Etacheri, V.; Marom, R.; Elazari, R.; Salitra, G.; Aurbach, D. Challenges in the development of advanced Li-ion batteries: a review. *RCS Energy Environ. Sci.* **2011,** *4* (9), 3243-3262.

(4) Wu, H.; Yu, G.; Pan, L.; Liu, N.; McDowell, M. T.; Bao, Z.; Cui, Y. Stable Li-ion battery anodes by in-situ polymerization of conducting hydrogel to conformally coat silicon nanoparticles. *Nature Communications* 4, Article number: 1943 (**2013**) doi:10.1038/ncomms2941

(5) Dimov, N.; Kugino, S.; Yoshio, M. Carbon-coated silicon as anode material for lithium ion batteries: advantages and limitations. *Elsevier Electrochimica Acta* **2003**, *48* (11), 1579-1587.

(6) de las Casas, C.; Li, W. A review of application of carbon nanotubes for lithium ion battery anode material. *Elsevier Journal of Power Sources* **2012**, *208*, 74-85.

(7) Zhang, Y.; Zhang, X. G.; Zhang, H. L.; Zhao, Z. G.; Li, F.; Liu, C; Cheng, H. M. Composite anode material of silicon/graphite/carbon nanotubes for Li-ion batteries. *Elsevier Electrochimica Acta* **2006**, *51* (23), 4994-5000.

(8) Cui, L.-F.; Yang, Y; Hsu, C.-M.; Cui, Y. Carbon-Silicon Core-Shell Nanowires as High Capacity Electrode for Lithium Ion Batteries. *ACS Nano Letters* **2009**, *9* (9), 3370-3374.

(9) Chon, M. J.; Sethuraman, V. A.; McCormick, A.; Srinivasan, V.; Guduru, P. R. Real-Time Measurement of Stress and Damage Evolution during Initial Lithiation of Crystalline Silicon. *Physical Review Letters* **2011**, *107* (4), 045503-1 - 045503-4.

(10) Saha, A.; Nikova, A.; Venkataraman, P.; John, V. T.; Bose, A. Oil Emulsification Using Surface-Tunable Carbon Black Particles. *ACS Applied Materials and Interfaces* **2013**, *5* (8), 3094-3100.

(11) Chen, Y.; Nie, M.; Lucht, B. L.; Saha, A.; Guduru, P. R.; Bose, A. High Capacity, Stable Silicon/Carbon Anodes for Lithium-Ion Batteries Prepared Using Emulsion-Templated Directed Assembly. *ACS Appl. Mater. Interfaces* **2014**, *6* (7), 4678-4683.

(12) Zhang, Y.; Pan, Y.; Chen, Y.; Lucht, B. L.; Bose, A. Towards reducing carbon content in silicon/carbon anodes for lithium ion batteries. *Elsevier Carbon* **2017**, *112*, 72-78.

(13) Saha, A.; Nikova, A.; Venkataraman, P.; John, V. T.; Bose, A. Oil Emulsification using Surface-Tunable Carbon Black Particles. *ACS Appl. Mater. Interfaces* **2013**, *5*, 3094-3100.

(14) Lim, S.; Kim, S.; Ahn, K. H.; Lee, S. J. The effect of binders on the rheological properties and the microstructure formation of lithium-ion battery anode slurries. *Elsevier Journal of Power Sources* **2015**, *299*, 221-230.

(15) Mustafa; Usui, H.; Ishizuki, M.; Shige, I.; Suzuki, H. R Rheological characteristics of non-spherical graphite suspensions. *Korea-Australia Rheology Journal* **2003**, *15* (1), 19-25

(16) Han, Z.-J.; Yabuuchi, N.; Shimomura, K.; Murase, M.; Yui, H.; Komaba, S. High-capacity Si-graphite composite electrodes with a self-formed porous structure by apartially neutralized polyacrylate for Li-ion batteries. *RCS Energy Environ. Sci.* **2012**, *5*, 9014-9020

(17) Singh, K. B.; Tirumkudulu, M. S. Cracking in Drying Colloidal Films. *APS Physical Review Letters* **2007**, *98*, 218302-1 – 218302-4

(18) Larson, R. G. The Structure and Rheology of Complex Fluids. *Oxford University Press New York*, 1999, Print, 13.

(19) Einstein, A. Eine neue Bestimmung der Moleküldimensionen. *Ann. Phys.* **1906**, *324* (2), 289-306.

MANUSCRIPT – II

Rheological Characterization of Graphite Lithium Ion Battery Anodes Containing Carbon Black

In preparation for submission to ACS Langmuir.

Joseph P. Sullivan, Arijit Bose

Chemical Engineering, University of Rhode Island, Kingston, RI, USA

Corresponding Author: Arijit Bose, Ph.D.

Chemical Engineering

University of Rhode Island

129 Pastore Hall, 51 Lower College Rd.

Kingston, RI, 02881, USA

Phone: +1-401-874-2804

Email address: bosea@uri.edu

Abstract

Lithium ion battery anodes are typically prepared from a slurry containing graphite, polyvinylidene fluoride, n-methyl-2-pyrrolidone, and small amounts of carbon black. Although carbon black accounts for only 1% of the anode's weight, the type used in the anode can have substantial effects on the viscoelastic properties of the slurry, affecting anode morphology, layer thickness, and efficiency. This study compared the viscoelastic properties of solutions containing Timcal Super P and Cabot LITX-50, two carbon black powders commonly used in graphite slurries. Super P appears to create a slurry that is easier to manufacture and less likely to suffer from cracks while drying than a slurry with LITX-50.

Introduction

Rechargeable lithium ion batteries (LIBs) are in high demand today, in part due to their favorable energy density as compared to other energy sources, and their promise as a potential replacement for internal combustion engines as vehicle power systems.[7,8] Graphite has long been used as an anode material for LIBs due to the ability of lithium ions to reversibly intercalate with a stoichiometry of LiC_6.[1] Carbon black can be added as a filler and conductive agent to increase performance and life cycle in LIBs.[2,4,5] The use of carbon black in a chemical vapor deposition process can reduce the number of pores present in graphite anodes, reducing the size of the solid electrolyte interface, thereby reducing the loss in first cycle capacity.[6]

In a typical manufacturing process, a slurry containing the active material, conducting carbon, binder, and solvent is first created. The slurry is then deposited either on a copper or aluminum film. Excess slurry is removed by a doctor blade. The slurry is then dried, calendared, and then sized. The rheological properties of the slurry have a strong impact on the thickness of the coated layer, as well as the morphology of the electrode during and after drying.[9,10] This study uses a stress controlled rheometer to determine how the addition of each component to the slurry affects the properties of the slurry as a whole.

Materials and Methods

Sample Preparation:

Polyvinylidene fluoride (PVDF), N-Methyl-2-pyrrolidone (NMP), industrial graphite, and Timcal Super P carbon black were provided by EaglePicher. LITX-50 carbon black was provided by Cabot. A 9:1 weight mixture of NMP to PVDF was created first, for use as a solvent for the remaining powder. This mixture was vortexed at 3000 rpm for 30 minutes in a sealed 20 ml vial and left to dissolve the remaining PVDF overnight. Graphite and carbon black were added to the solution such that 91% of the final solid mass was graphite, 2% was CB, and 7% was PVDF. The CB added was either Timcal Super P or Cabot LITX-50, as indicated in individual results. Additional NMP was added until the total mass of NMP was equal to the total mass of solid components. This slurry was vortexed at 3000 rpm for 20 minutes until homogeneous.

Rheology:

Characterization was completed by a TA Instruments AR-2000 stress controlled rheometer. As the particles in solution were much smaller than 10 μm, a cone and plate geometry was utilized. This configuration had a set minimum gap height of 51 μm, a cone angle of 2°, and a cone diameter of 4 cm. All experiments were completed at 25 C.

Samples were first probed for a change in viscosity with respect to shear rate, ranging from 3 s^{-1} to 2000 s^{-1}. Each experiment began with a preshear of 10 s^{-1} for 120

seconds to remove stresses incurred during sample loading. Viscosity characterization was performed three times for each sample.

Some samples were also probed for viscoelastic response. A logarithmic sweep of the torque range of the instrument at 1 Hz was the method of determining the linear viscoelastic region for the samples. Once the LVR was determined, all samples were agitated for a minimum of 20 seconds, and each sample was probed within three minutes. A 0.1 rad/s preshear was utilized for the oscillatory sweep. Storage (G') and loss (G") moduli were calculated for increasing angular frequency at an oscillatory stress within the linear viscoelastic region. This covered an angular frequency range of 0.01 to 100 rad/s.

Results and Discussion

NMP/PVDF Solvent:

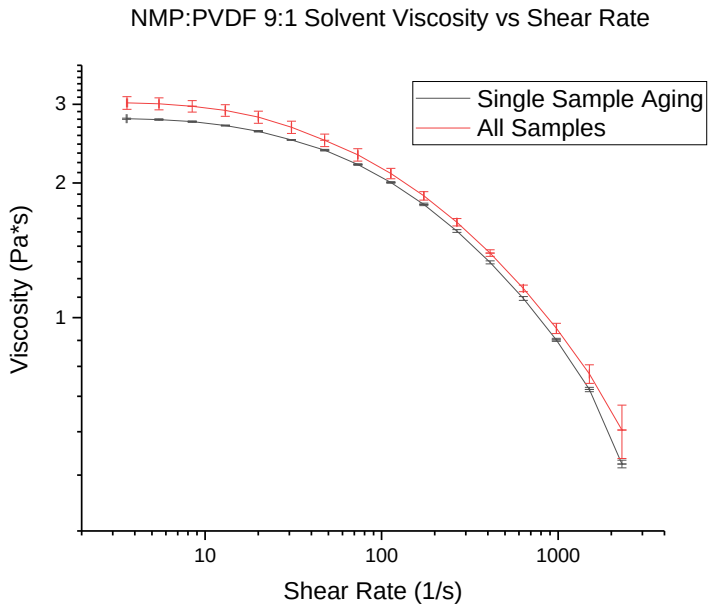

Fig. 16: Short-term aging of the solvent and viscosity for all samples

Characterization began with the 9:1 mixture of NMP and PVDF used as a solvent for the graphite and carbon black. First, the viscosity of the solvent was determined as a function of shear rate. Three sequential shear rate sweeps were performed on one sample, five minutes apart, to determine the short term aging of the sample, shown as the black line in Figure 16. The low variance in these results increases confidence that the system has been mixed properly, with little aging present.

Multiple shear rate sweeps were then completed for samples from the first vial to determine variability within a batch of samples, and subsequent vials were compared against this data for consistency, shown as the red line in Figure 16. All

subsequent results in this manuscript use the NMP/PVDF mixture as a solvent; the low error present in sample preparation increases confidence in the results. An apparent zero-shear viscosity is present at ~ 3 Pa*s for the NMP/PVDF mixture, which yields to shear thinning behavior at low shear rate.

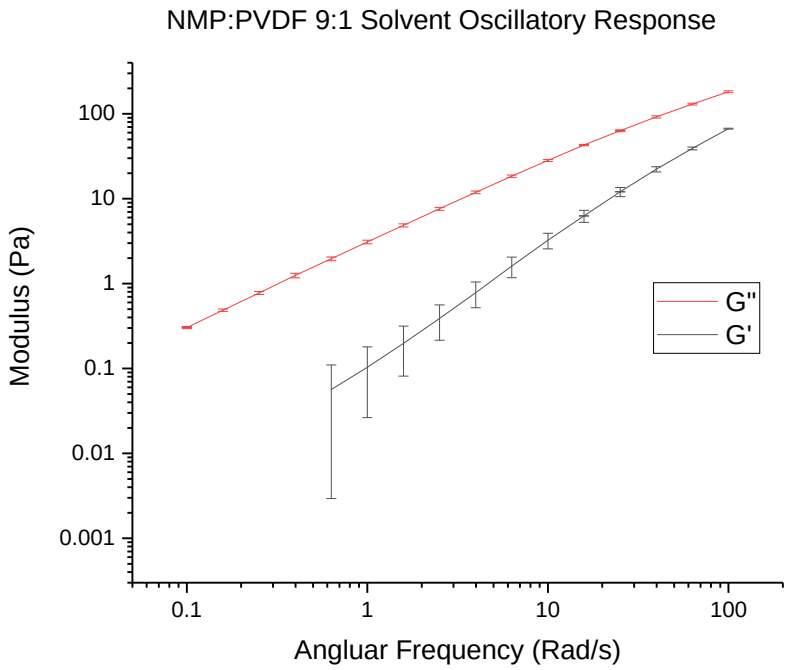

Fig 17. Moduli of NMP/PVDF solvent, 1 Pa osc. stress

The solvent modulus, Fig.17, in conjunction with the LVR behavior, (not shown), is typical of an elastic fluid, namely, a polymer melt in solution. The loss modulus (G") increases at a faster rate than the storage modulus, indicating that the elastic nature of the material is slowly being overcome, as the rate of deformation increases.

Carbon Black and Solvent:

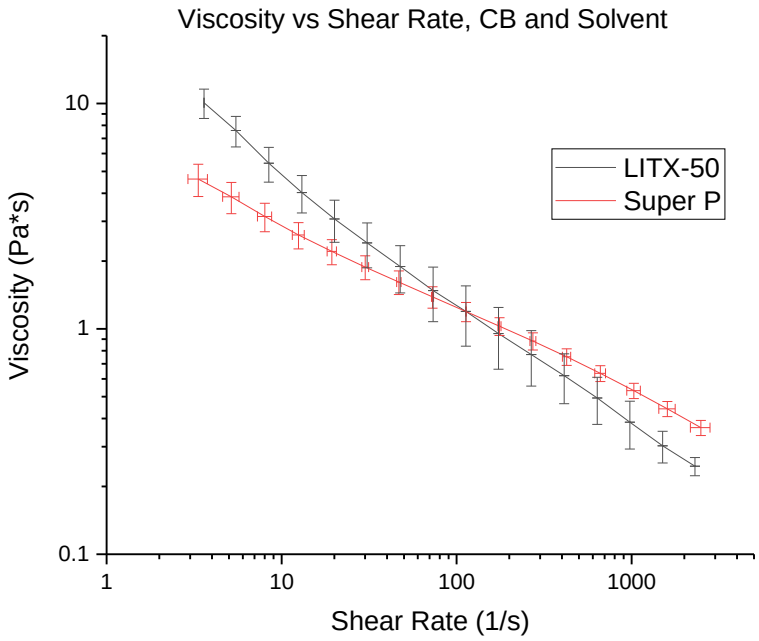

Fig. 18: Viscosity of solvent and two carbon black additives

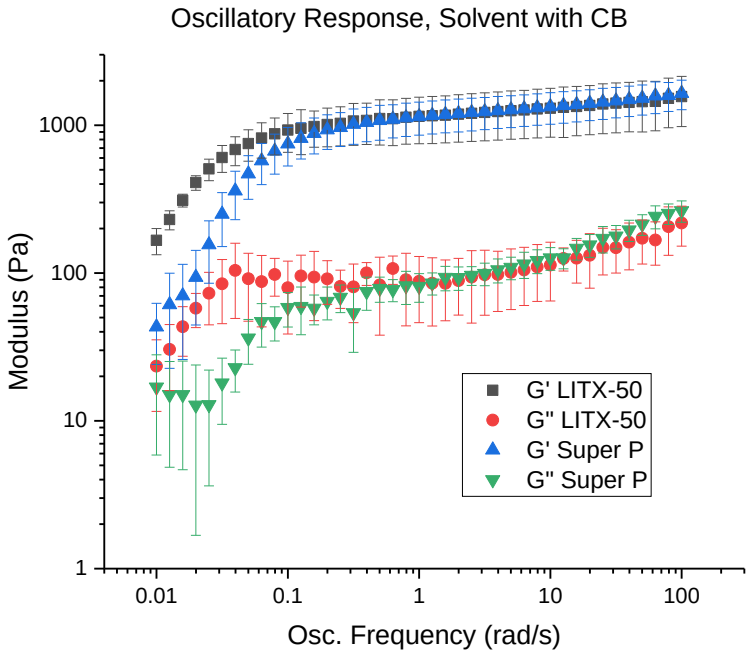

Fig. 19: Moduli of solvent and two carbon black additives, 1 Pa. oscillatory stress

Once the base solvent was characterized, 2 wt% CB was added to the NMP/PVDF mixture. As with the base solvent, viscosity was measured for each prepared sample vial to confirm consistency among samples. This shear thinning behavior seen in Fig. 18, in contrast to the solvent, does not show a low shear viscosity plateau before a yield. The addition of 2 wt% of either CB increased the low shear viscosity of the solvent substantially, but also rapidly increased the rate of shear thinning. Although both CB solutions thin to 1 Pa*s at a shear rate of 100 s^{-1}, the solvent reaches 1 Pa*s at 1,000 s^{-1}. The modulus response for each form of CB is that of a highly structured fluid.

Graphite Slurries:

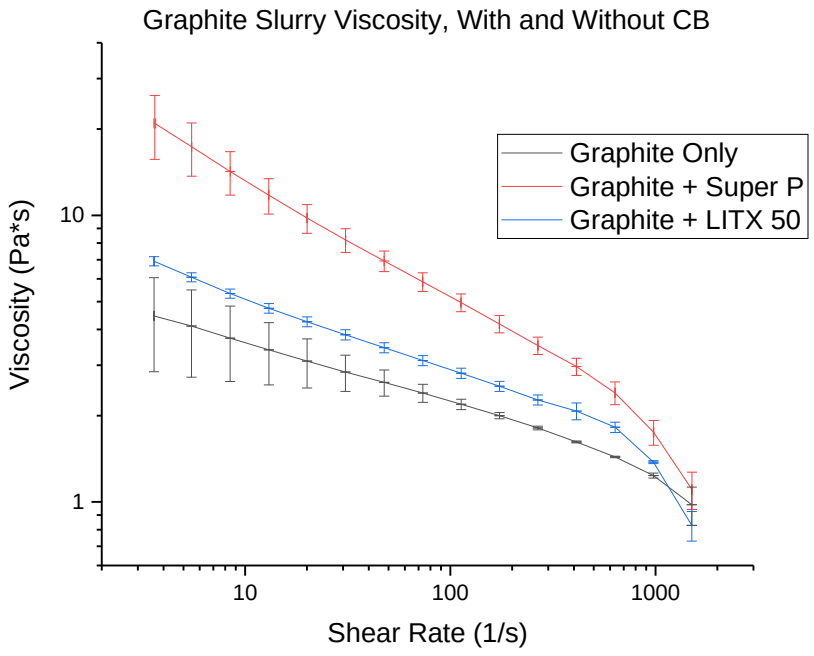

Fig. 20: Graphite slurry viscosity, with and without CB

Solution viscosity after addition of graphite powder to the solvent, with and without CB, is shown in Fig. 20. The addition of Super P to a system that includes graphite increases the viscosity considerably.

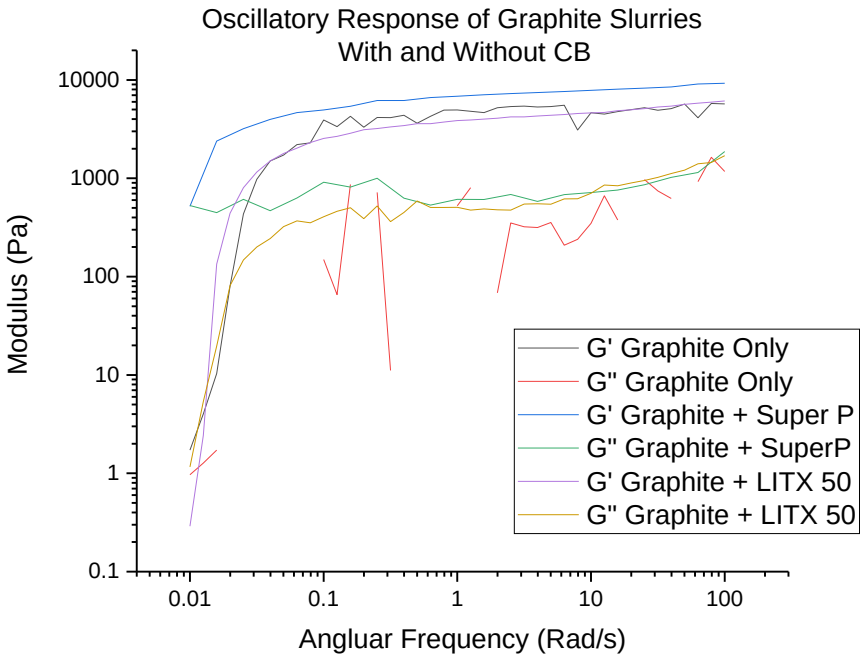

Fig. 21: Moduli for graphite slurries with and without CB

All oscillatory measurements for solvent with graphite and carbon black were taken at 1 Pa oscillatory stress. A notable result is the lack of a stable LVR for the graphite slurry. The most stable portion, 1 Pa, was chosen for oscillatory characterization. Fig. 21 illustrates this instability; there is no reliable G" response (red line) for the sample with solvent and graphite. This behavior is consistent with solid-like composite materials, which are particularly susceptible to instability.

The increased storage modulus of the Super P implies that at low shear rates, the fractal network of the CB remains intact. This is shown by the increases in modulus and viscosity of Super P as compared to LITX-50 at the same shear rate. A

transition is present within the range of 100 s^{-1} to 1000 s^{-1} shear rate and frequency for the viscosity and inelastic modulus data, respectively. Around this value, both CB samples become considerably more inelastic, and increase the degree of shear thinning.

Conclusions

The rheological characteristics of lithium ion battery anode slurries containing PVDF, NMP, graphite, and one of two carbon black formulations have been presented. A 9:1 mixture of NMP:PVDF, used as the solvent for the carbon components, presents a yield stress of around 3 Pa*s, behavior expected of a polymer. The addition of carbon black removed this yield stress, altering the fluid behavior to that of a power law fluid without Newtonian plateaus. The parallel G' and G" values, as shown from the oscillatory response, are a characteristic of a weak particulate gel. Gelation increases when graphite is added to the slurry: both moduli increase, with G" increasing substantially. The Timcal Super P appears to provide a stronger network, due to larger storage modulus, and has more shear thinning behavior than the Cabot LITX-50. Both behaviors are beneficial for manufacturing, assuming the electrochemical properties of the completed anode do not suffer. A more structured gel can more efficiently absorb the stresses of drying without cracking, and a gel with a greater degree of shear thinning behavior can be manipulated more precisely by a doctor blade to control coating thickness.

References

(1) Yoshio, M.; Wang, H.; Fukuda, K.; Hara, Y.; Adachi, Y. Effect of Carbon Coating on Electrochemical Performance of Treated Natural Graphite as Lithium-Ion Battery Anode Material. *J. Electrochem. Soc.* **2000**, *147* (4), 1245-1250

(2) Wu, H.; Yu, G.; Pan, L.; Liu, N.; McDowell, M. T.; Bao, Z.; Cui, Y. Stable Li-ion battery anodes by in-situ polymerization of conducting hydrogel to conformally coat silicon nanoparticles. *Nature Communications* 4, Article number: 1943 (**2013**) doi:10.1038/ncomms2941

(3) Etacheri, V.; Marom, R.; Elazari, R.; Salitra, G.; Aurbach, D. Challenges in the development of advanced Li-ion batteries: a review. *RCS Energy Environ. Sci.* **2011,** *4* (9), 3243-3262.

(4) Luo, Y.-N.; Tsai, Y.-T.; Lin, K.-H. The influence of added nano carbon black on the electrical properties of a lithium-ion secondary battery. *Journal of Ceramic Processing Research* **2016**, *17* (10), 1082-1087

(5) Fransson, L.; Eriksson, T.; Edström, K.; Gustafsson, T.; Thomas, J. O. Influence of carbon black and binder on Li-ion batteries. *Elsevier Journal of Power Sources* **2001**, *10* (1), 1-9

(6) Natarajan, C.; Fujimoto, H.; Tokumitsu, K.; Mabuchi, A.; Kasuh, T. Reduction of the irreversible capacity of a graphite anode by the CVD process. *Elsevier Carbon* **2001**, *39* (9), 1409-1413

(7) Scrosati, B.; Garche, J. Lithium batteries: Status, prospects and future. *Elsevier Journal of Power Sources* **2010**, *195* (9), 2419-2430

(8) Goodenough, J.; Park, K.-S. The Li-Ion Rechargeable Battery: A Perspective. *J. Am. Chem. Soc.* **2013**, *135* (4), 1167-1176.

(9) Scherer, G. W. Theory of Drying. *J. Am. Ceram. Soc.*, **1990**, *73* (1), 3-14.

(10) Yoo, M.; Frank, C. W; Mori, S. Interaction of Poly(vinylidene fluoride) with Graphite Particles. 1. Surface Morphology of a Composite Film and Its Relation to Processing Parameters. *Chem. Mater.*, **2003**, *15* (4), 850-861.

MANUSCRIPT – III

Rheological Characterization of Block-Co-Polymer Solutions Containing Thermal Accelerant

In preparation as part of a larger study of thermal accelerant solutions, to be submitted to Theranostics.

Joseph Patrick Sullivan[1], William Keun Chan Park[2], Michael Patrick Primmer[2],

[1]Department of Chemical Engineering, University of Rhode Island, Kingston, RI, USA

[2]Department of Diagnostic Imaging, Rhode Island Hospital, The Warren Alpert Medical School of Brown University, Providence, Rhode Island, USA

Corresponding Author: Joseph P. Sullivan

Chemical Engineering

The University of Rhode Island

129 Pastore Hall, 51 Lower College Rd.

Kingston, RI, 02881, USA

Phone: +1-401-644-6508

Email address: josephsullivan@uri.edu

Abstract

Rheological characterization and viscosity measurements were made for several thermal accelerant solutions. Thermal accelerant is designed to deliver as a solution into the liver with sufficient viscosity to remain stationary at a target site during ablation. After the rheological characterization of a series of the thermal accelerant solutions, the sample designated “TA 50” appears to meet these criteria most effectively.

Introduction

Hepatic cancers are the fifth most common cancer in men and eighth most common in women worldwide.[1] Image-guided thermal ablation (IGTA) including radiofrequency or microwave as energy sources, has long been used as a method of treatment for hepatic cancer. [2-5] RFTA is a process through which an electrode is percutaneously inserted into the liver and an RF generator provides energy, dissipated locally in the form of heat, to destroy cancer cells.[4] For treatment of tumors larger than 3 cm, RFTA is considerably more effective than any other method, including percutaneous ethanol injection.[4] Motivation for the development of a new treatment arose from the prevalence of liver cancer, and low rates of success in treatments such as chemotherapy and radiation therapy. By some calculations, there is an 80% 5-year recurrence rate from surgery alone.[5]

In contrast to RFTA, which relies on an electrical current to destroy tumors, microwave ablation (MWA) uses an electromagnetic field to excite water molecules, generating heat locally.[8] The mechanism for MWA is faster than RFTA and produces a larger, more homogeneous area of ablation.[9,10] Despite its advantages, thermal ablation has shown a tumor recurrence rate of 30%, mainly due to incomplete ablation.[6] The auxiliary application of a microwave responsive thermal accelerant may increase the effectiveness of thermal ablation treatments. This application, guided by CT or ultrasound, augments the microwave energy in the area of the antenna to expand the treatment area. Without thermal accelerant, tumors not spherical in nature would typically require several targeted treatments.[3,6] Additionally, many liver tumors are

located near large blood vessels; the application of a thermal accelerant adjacent to the blood vessel blocks the cooling effect of the rapid blood flow during treatment, thereby achieving complete ablation.

The thermal accelerant is delivered to the liver as a mixture containing a structurally modified biopolymer. One necessary property of the polymer is the ability to remain stationary at the target site as it is injected. The optimal viscosity limits the movement of the liquid once inside the body and prevents unintentional damage to the tissue surrounding the tumor. To determine the viability of a sample, a rheometer is used to simulate the shear conditions and temperatures present during operating conditions. Rheological characterization of various biopolymer mixtures can quantify their respective viscosities during injection, their behavior once in the body, and the temperatures at which their viscosity greatly increases and gelation occurs.

In this study, biopolymer mixtures containing various concentrations of polymer and thermal accelerant were characterized using a stress controlled rheometer over a range of shear rates, simulating conditions inside the body (1-100 s^{-1}) and during injection (100-1,000 s^{-1}). For samples that were sufficiently non-Newtonian, viscoelastic moduli were determined. These results were analyzed and used to determine the most effective formulation of thermal accelerant for thermal ablation.

Materials and Methods

Sample Preparation:

Thermal accelerant samples were prepared in the molecular imaging lab of the Warren Alpert Medical School of Brown University. Varying amounts of thermal accelerant was added to different biopolymer solutions, the contents of which are not yet available in the public domain.

Rheology:

Characterization was completed by a TA Instruments AR-2000 stress controlled rheometer. A cone and plate geometry was utilized. This configuration had a set minimum gap height of 51 μm, a cone angle of 2°, and a cone diameter of 4 cm. This gap is much larger than the minimum particle size. All experiments were done at 25 °C.

Samples were first probed for a change in dynamic viscosity with respect to shear rate, ranging from 3 s^{-1} to 2000 s^{-1}. Each experiment began with a preshear of 10 s^{-1} for 120 seconds to remove stresses incurred during sample loading. Viscosity characterization was performed three times for each sample.

Some samples were also probed for viscoelastic response. A determination of the appropriate range of oscillatory stress for each sample is required before oscillatory response can be obtained. Within this range, called the linear viscoelastic region (LVR), the viscoelastic properties are independent of stress or strain levels. A

logarithmic sweep of the torque range of the instrument at 1 Hz was the method of determining the linear viscoelastic region for the samples. Once the LVR was determined for a sample, it was agitated for 30 seconds, and each sample was probed within three minutes. A 0.1 rad/s preshear was utilized for the oscillatory sweep. For this application, the dynamic sweep covered a range of 1 to 100 rad/s, at a temperature of 25 ^{o}C.

Additionally, viscosity response with increasing temperature was relevant for several samples. For these temperature sweeps, the temperature was increased from 50 ^{o}C to 75 ^{o}C at a rate of 5 ^{o}C/min and a constant shear rate of 2.85 s^{-1} throughout.

Results and Discussion

Oscillatory Response:

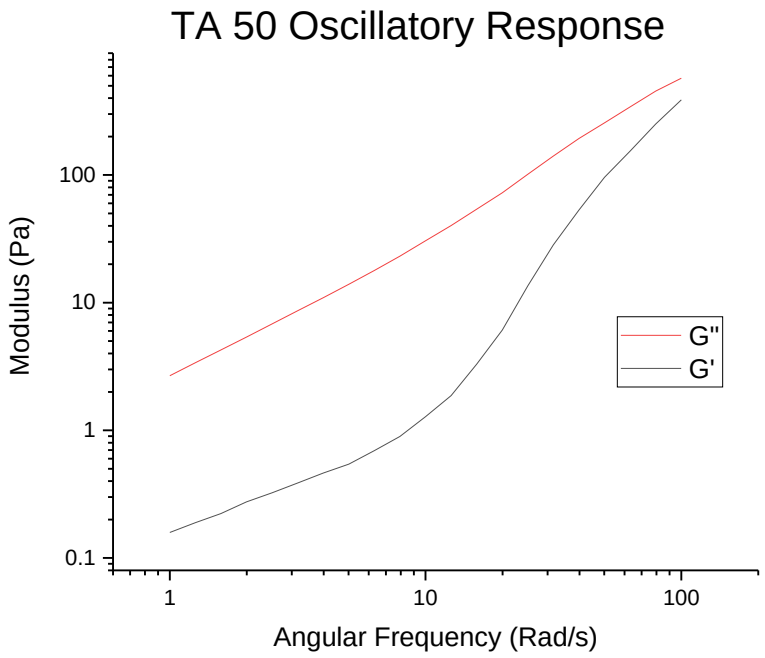

Fig. 22: Moduli for TA 50, 1 Pa oscillatory stress.

Of the samples for which an LVR measurement was attempted, only TA 50 exhibited a stable LVR at 25 ºC. The oscillatory response of TA 50 is shown in Fig. 22. As G" is larger than G', and the theoretical point at which the two will cross is at an angular frequency greater than 100 rad/s, this fluid can be characterized as a weak polymer melt. This result indicates that an extremely weak gel is present in the solution at 25 ºC, although the block-co-polymer is designed to form a gel between 34 ºC and 39 ºC.

Temperature Dependent Viscosity:

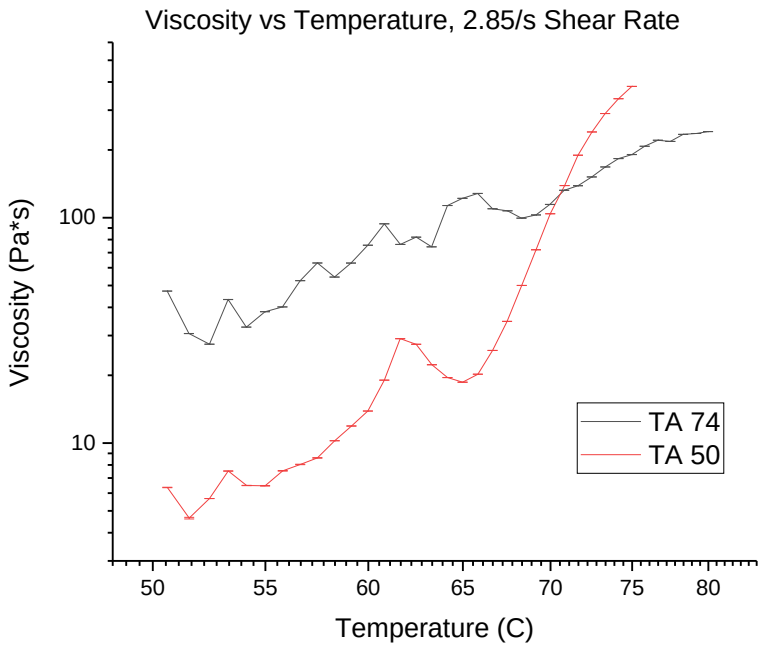

Fig. 23: Temperature dependence of viscosity for two TA solutions, constant shear rate

A phase transition is desired in the copolymer system at 60 ^{o}C to separate polymeric precipitate and water. Figure 23 shows the viscosity response of two compounds at a low shear rate. The viscosity increase with temperature is much more prevalent in the TA 50 sample than the TA 74 sample. A viscosity increase of nearly two orders of magnitude is observed for TA 50 as temperature increases from 50 ^{o}C to 75 ^{o}C, while TA 74 increases about tenfold. There is a clear increase in viscosity for TA 50 around 60 ^{o}C, followed by a decrease and another, more pronounced increase in the next 10 ^{o}C temperature range. This sharp viscosity decrease is likely due to the temperature stratification present between the heated stationary plate and the unheated rotating cone of the rheometer. As the phase transition begins to precipitate polymer

from the mixture, the viscosity decreases until the precipitate begins to interfere with the flow of water/polymer mixture above it.

Viscosity vs Shear Rate:

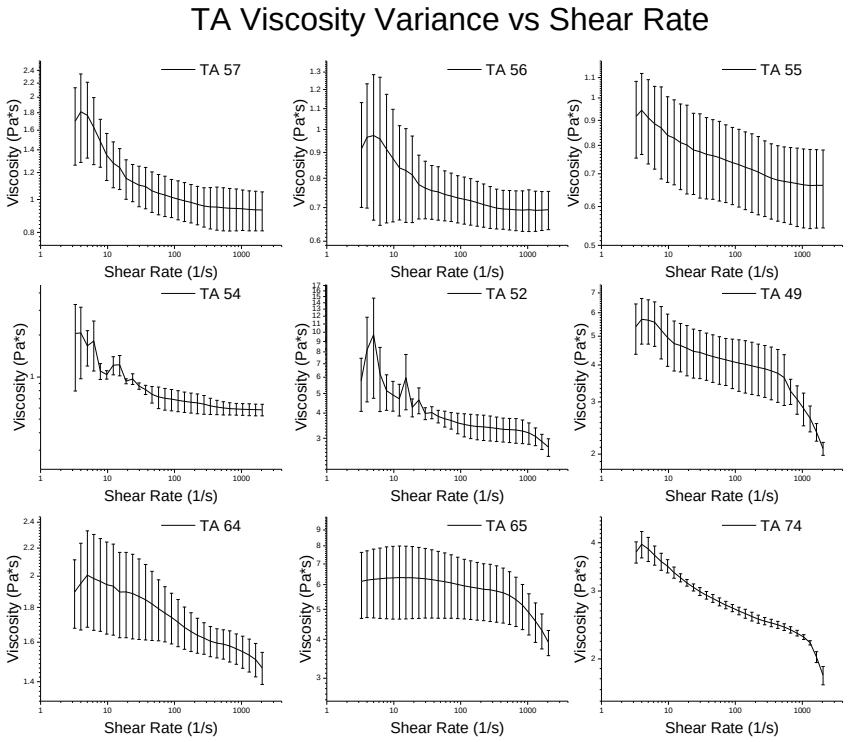

Fig. 24: Viscosity sweeps of several TA solutions

In addition to the previous TA 50 and TA 74 results, viscosity response to increasing shear rate was determined for several TA mixtures. Results are presented in figure 24.

Conclusions

Within the constraints inherent in microwave thermal ablation, the TA 50 polymer formulation shows promise as a base for an effective thermal accelerant. The TA 50 solution behaves like a weak gel at 25 ^{o}C and undergoes a one and one half order of magnitude increase in viscosity between 65 ^{o}C and 75 ^{o}C. These properties suggest that the solution will inject into the liver as a liquid with low viscosity, form a gel at body temperature, and begin to precipitate the polymer from solution around 60 ^{o}C, as is required for MWA.

References

(1) Bosch, F. X.; Ribes, J.; Díaz, M.; Cléries, R. Primary liver cancer: Worldwide incidence and trends. *AGA Gastroenterology* **2004**, *127* (5), S5-S16.

(2) Lin, S.-M.; Lin, C.-J.; Lin, C.-C.; Hsu, C.-W.; Chen, Y.-C. Randomised controlled trial comparing percutaneous radiofrequency thermal ablation, percutaneous ethanol injection, and percutaneous acetic acid injection to treat hepatocellular carcinoma of 3 cm or less. *Gut* **2005**, *54*, 1151–1156. doi: 10.1136/gut.2004.045203

(3) Lencioni, R. A.; Allgaler, H.-P.; Cioni, D.; Olschewski, M.; Delbert, P.; Crocetti, L.; Frings, H.; Laubenberger, J.; Zuber, I.; Blum, H. E.; Bartolozzi, C. Small Hepatocellular Carcinoma in Cirrhosis: Randomized Comparison of Radio-frequency Thermal Ablation versus Percutaneous Ethanol Injection. *Radiology* **2003**, *228*, 235-240. doi: 10.1148/radiol.2281020718

(4) Livraghi, T.; Lazzaroni, S.; Meloni, F. Radiofrequency thermal ablation of hepatocellular carcinoma. *Elsevier European Journal of Ultrasound* **2001**, *13*, 159-166

(5) Rossi, S.; Di Stasi, M.; Buscarini, E.; Quaretti, P.; Garbagnati, F.; Squassante, L.; Paties, C. T.; Silverman, D. E.; Buscarini, L. Percutaneous RF Interstitial Thermal Ablation in the Treatment of Hepatic Cancer. *American Journal of Roentgenology* **1996**, *167*, 759-768

(6) Park, W. K. C.; Maxwell, A. W. P.; Frank, V. E.; Primmer, M. P.; Paul, J. B.; Susai, C.; Collins, S. A.; Borjeson, T. M.; Baird, G. L.; Lombardo, K. A.; Dupuy, D. E. A novel thermal accelerant for augmentation of microwave energy during image-guided tumor ablation. Proc. SPIE 1066, Energy-Based Treatment of Tissue and Assessment IX **2017**, 10066 (02). doi:10.1117/12.2249772

(7) Brownsey, G. J.; Noel, T. R; Parker, R.; Ring, S. G. The Glass Transition Behavior of the Globular Protein Bovine Serum Albumin. Biophysical Journal **2003**, 85 (6), 3943-3950

(8) Poulou, L. S.; Botsa, E.; Thanou, I.; Ziakas, P. D.; Thanos, L. Percutaneous microwave ablation *vs* radiofrequency ablation in the treatment of hepatocellular carcinoma. *World Journal of Hepatology* **2015**, **7** *(8)*, 1054-1063

(9) Simon, C. J.; Dupuy, D. E.; Mayo-Smith, W. W. Microwave ablation: principles and applications. *Radiographics* **2005**, **25** Suppl 1:S69-S83

(10) Lloyd, D. M.; Lau, K. N.; Welsh, F.; Lee, K. F.; Sherlock, D. J.; Choti, M. A.; Martinie, J. B.; Iannitti, D. A. International multicentre prospective study on microwave ablation of liver tumours: preliminary results. *HPB* (Oxford) **2011**, **13**, 579-585